NOTAS DE FÍSICA

VOLUME XII

Nº 12

ANGULAR DISTRIBUTION IN PION ELECTROPRODUCTION

by

N. Zagury

CENTRO BRASILEIRO DE PESQUISAS FÍSICAS

Av. Wenceslau Braz, 71

RIO DE JANEIRO

1967

Notas de Física - Volume XII - Nº 12

ANGULAR DISTRIBUTION IN PION ELECTROPRODUCTION *

N. Zagury **
Physics Department
Harvard University, Cambridge, Massachusetts

(Received March 10, 1967)

I. INTRODUCTION

Recently the Cornell group [1] has observed the reactions:

$$e^- + p \rightarrow \begin{cases} e^- + p + \pi^0 \\ e^- + n + \pi^+ \end{cases} \qquad (1)$$

by detecting two charged particles in coincidence. Experiments of this kind open up the possibility of studying the angular distribution of pions in the transverse, longitudinal and in the interference contributions to the cross section [2]. In particular one can study the relative importance of the several multipoles involved and their possible resonance behaviour [3]. Also, as was

* Supported in part by the Office of Naval Research under contract Nonr-1866(55).

** On leave of absence from "Centro Brasileiro de Pesquisas Físicas" and "Faculdade Nacional de Filosofia" - Rio de Janeiro - Brazil.

pointed out by Frazer [4] the study of the π^+-angular distribution can lead, through an extrapolation procedure, to a value of the pion form factor.

Dispersion relation techniques have been used with some success in the description of reaction (1) in the region of the first resonance of the π-N system. [5,6] It is assumed that the most important effects can be taken in account by the Born terms and the resonant magnetic transition to the (3-3) final state. Recently, this author [6] has considered a solution for the (3-3) amplitudes which is cut-off independent and includes recoil corrections. Also, a full relativistic treatment of the Born terms was made and corrections to the E_{o+} and M_{1-} amplitudes due to the disperison integrals were considered. This paper is an extension of A. We have used the results of A to calculate the angular distribution of the pions for the different contributions to the cross section. Also we have analysed the variations on these angular distributions when we change the pion form factor. It is found that the shape of the longitudinal π^+-cross section is quite sensitive to this quantity. The effect of adding ω and ρ exchange was considered. Their contribution was found small for the range of energies and momentum transfer considered and of the order of other uncertainties in the theory.

II. GENERAL RESULTS

Let k_1, k_2, p_1, p_2 and q denote the initial and final electron momenta, the initial and final nucleon momenta and the pion momentum, respectively. The masses of nucleon, electron and pion will be called m, m_e, and μ respectively. The 4-momentum transfer[7] given up by the electron will be called λ^2. The invariant T-matrix is defined by:

$$S_{fi} = \delta_{fi} + (2\pi)^4 \, \delta^4(k+p_1-p_2-q)\left[\frac{m_e^2 \; m^2}{k_{10}k_{20}p_{10}p_{20}2q_o}\right]^{\frac{1}{2}} T \quad (2.1)$$

where $k = k_1 - k_2$. To first order in the electromagnetic coupling the process is described by diagram in fig. 1 and we can write:

$$T = \epsilon_\mu \, j^\mu \quad (2.2)$$

where

$$\epsilon_\mu = \frac{1}{\lambda^2} \, \bar{u}(k_2) \, \gamma_\mu \; u(k_1) \quad (2.3)$$

is the leptonic current times the photon propagator and j_μ is the hadronic current.

The T-matrix can be written in terms of the center of mass amplitudes $\mathcal{F}_i$ as:

$$T = \frac{4\pi W}{m} \chi^+ \left[i\mathcal{F}_1 \vec{\sigma}\cdot\vec{\epsilon} + \mathcal{F}_2 \frac{\vec{\sigma}\cdot\vec{q} \; \vec{\sigma}\cdot\vec{k}\times\vec{\epsilon}}{qk} + i\mathcal{F}_3 \frac{\vec{\sigma}\cdot\vec{k} \; \vec{q}\cdot\vec{\epsilon}}{qk} + i\mathcal{F}_4 \frac{\sigma\cdot\vec{q} \; \vec{q}\vec{\epsilon}}{qk} \right.$$

$$\left. + i\mathcal{F}_5 \frac{\vec{\sigma}\cdot\vec{k} \; \vec{k}\cdot\vec{\epsilon}}{k^2} + i\mathcal{F}_6 \frac{\vec{\sigma}\cdot\vec{k} \; \vec{q}\vec{\epsilon}}{qk} - i\mathcal{F}_7 \frac{\vec{\sigma}\cdot\vec{q}}{q} \epsilon_o - i\mathcal{F}_8 \frac{\vec{\sigma}\cdot\vec{k}}{k} \epsilon_o \right] \quad (2.4)$$

where the χ's are Pauli spinors, k and q are the nucleon initial and final momenta and W is the total energy in the center of mass

system. The expansion of the $\mathcal{F}$'s into multipoles amplitudes is given in A.

The $\mathcal{F}$'s are considered to be the sum of four contributions:

$$\mathcal{F} = \mathcal{F}^B + \mathcal{F}^R_{3,3} - \mathcal{F}^B_{3,3} + \mathcal{F}^{cor} \qquad (2.5)$$

$\mathcal{F}^B$ is given by the Born diagrams of fig. 2, $\mathcal{F}^R_{3,3}$ is the resonant T = 3/2, J = 3/2 contribution, $\mathcal{F}^B_{3,3}$ is the T = 3/2, J = = 3/2 component of the Born term that should be subtracted off the full $\mathcal{F}^B$ and $\mathcal{F}^{cor}$ is the correction to the E_{0+} and M_{1-} multipoles introduced by considering the imaginary part of the amplitudes in the fixed - t dispersion relations as being given by the imaginary part of the (3-3) amplitudes. In A we have considered in detail those contributions. The results for the magnetic M_{1+}, electric E_{1+} and scalar S_{1+} transitions to the (3,3) final state were [8]

$$M_{1+} = M^B_{1+,\pi}\, e^{i\delta}\cos\delta + \Big[0{,}036(e/f)\, C_1(\lambda^2)\, F_\pi(\lambda^2) + 2.87(e/f)\, C(\lambda^2)\mu/2m \times \times G_{MV}(\lambda^2)\Big]\, \frac{e^{i\delta}\sin\delta}{q^2}\, \frac{kW}{\sqrt{(E_1+m)(E_2+m)}} \qquad (2.6)$$

$$E_{1+} = E^B_{1+,\pi}\, e^{i\delta}\cos\delta - 0.013(e/f)C_2(\lambda^2)\, F_\pi(\lambda^2)\, \frac{e^{i\delta}\sin\delta}{q^2}\, \frac{kW}{\sqrt{(E_1+m)(E_2+m)}} \qquad (2.7)$$

$$S_{1+} = S^B_{1+\pi} e^{i\delta}\cos\delta - 0.084(e/f)C_3(\lambda^2)\, F_\pi(\lambda^2)\, \frac{e^{i\delta}\sin\delta}{q^2}\, \frac{k^2}{\sqrt{(E_1+m)(E_2+m)}} \qquad (2.8)$$

where $M^B_{1+,\pi}$, $E^B_{1+,\pi}$, $S^B_{1+,\pi}$ denote the magnetic, electric and scalar multipoles projected out of the meson-pole diagram in fig. 2C, $F_\pi(\lambda^2)$ and $G_{MV}(\lambda^2)$ are the pion form factor and the magnetic isovector form factor normalized to 1, δ is the π-N phase shift for the $T = 3/2$, $J = 3/2$ state and the C's are given by:

$$C(\lambda^2) \approx 1/(1 - \lambda^2/(2.4)^2) \tag{2.9}$$

$$C_1 \begin{cases} \sim 1 & \text{for } -0.1 < \lambda^2 < 0 \\ \approx (1.11 - 0.16\,\lambda^2)/(1 - 1.51\lambda^2) & \text{for } \lambda^2 < -0.1 \end{cases} \tag{2.10}$$

$$C_2 \approx \begin{cases} 1 - 2.55\,\lambda^2 - 5.2\,\lambda^4 & \text{for } -0{,}3 < \lambda^2 < 0 \\ (1.59 - 0.12\lambda^2)/(1 - 0.91\lambda^2) & \text{for } \lambda^2 < -0{,}3 \end{cases} \tag{2.11}$$

$$C_3 \approx \begin{cases} 1 - 7.47\lambda^2 - 31.3\lambda^4 & \text{for } -0.16 < \lambda^2 < 0 \\ (1.98 - 0.26\,\lambda^2)/(1 - 2.83\lambda^2) & \text{for } \lambda^2 < -0.16 \end{cases} \tag{2.12}$$

where λ^2 is given in Bev^2.

$\mathcal{H}^{cor}$ was given in section V of A. The ω and ρ - exchange were not included in A. Here we consider the ω and ρ as stable particles. The contribution from the diagrams in fig. 3 to the T-matrix is given by:

$$\frac{g_{\pi\gamma\rho}}{m_\rho}\,\epsilon^{\mu\nu\tau\lambda}\,\epsilon_\mu\,k_\nu q_\tau\,\bar{u}(p_2)\left[G_{1\rho}\,\gamma_\lambda + i\,G_{2\rho}/2m\;\sigma_{\lambda\beta}(p_2 - p_1)^\beta\right]u(p_1) \times$$

$$\times \frac{\gamma_\alpha}{t - m_\rho^2} + \frac{g_{\pi\gamma\omega}}{m_\omega}\,\epsilon^{\mu\nu\tau\lambda}\,\epsilon_\mu\,k_\nu\,q_\tau\,\bar{u}(p_2)\left[G_{1\omega}\gamma_\lambda + iG_{2\omega}/2m\;\sigma_{\lambda\beta}(p_2 - p_1)^\beta\right]u(p_1) \times$$

$$\times \frac{\delta_{3\alpha}}{t - m_\omega^2} \tag{2.13}$$

Were α is the isotopic spin label of the outgoing pion. The NNρ and NNω couplings $G_{1\rho}$, $G_{2\rho}$, $G_{1\omega}$, $G_{2\omega}$ were taken from the Ball, Scotti and Wong [9] analysis of the nucleon-nucleon problem. $g^2_{\pi\gamma\omega}$ was obtained from the experimental width [10] $\Gamma_{\omega \to \pi+\gamma}$. $g_{\pi\gamma\rho}$ was estimated [11] as 1/3 $g_{\pi\gamma\omega}$ according to the quark model. This value for $g_{\pi\gamma\rho}$ is not in disagreement with estimates based on the ratio of π^- and π^+ photo-production cross-sections [12] at threshold or measurements [13] of an upper limit for $\Gamma_{\rho \to \pi+\gamma}$.

As it was expected these terms do not contribute much in the region of energies and momentum transfer we have considered. The deviations from the values in the case $G_{1\rho} = G_{2\rho} = G_{1\omega} = G_{2\omega} = 0.0$ are much smaller than those due to other uncertainties in the theory like precise values for G_{eN} and F_π. Therefore, from now on we will neglect those terms.

III. CROSS SECTION

In the lowest order on the electromagnetic coupling the differential cross section can be written as [1,2]:

$$\frac{d\sigma}{d\Omega_e^L \, dk_{2e}^L \, d\Omega_\pi} = \Gamma \left\{ W_1(\theta) + \epsilon \sin^2\theta \cos 2\varphi \; W_2(\theta) \right.$$

$$\left. + \sqrt{\frac{\epsilon(\epsilon+1)}{2}} \sin\theta \cos\varphi \, W_3(\theta) + W_4(\theta) \right\} \qquad (3.1)$$

$$\Gamma = \frac{e^2}{8\pi^2} \frac{k_2^L}{m \, k_1^L} \frac{Wk}{(-\lambda^2)} \frac{1}{1-\epsilon} \qquad (3.2)$$

where the upperscript "L" means Laboratory System, θ and φ are the polar and azymuthal nucleon scattering angle in the center of mass system and ϵ is given by:

$$\epsilon = \frac{\frac{-\lambda^2}{2W^2k^2}\ \cot g^2\frac{\alpha}{2}}{1 - \frac{\lambda^2}{2W^2k^2}\cot g^2\frac{\alpha}{2}} \tag{3.3}$$

α being the electron scattering angle in the lab system. W_1, W_2, W_3 and W_4 are functions of W, λ^2 and θ only. W_1 and W_2 contain only transverse contributions, W_4 only longitudinal contributions and W_3 contains the contributions from the interference between the transverse and longitudinal terms. At $\lambda^2 = 0$, W_3 and W_4 vanish. $W_1 + \epsilon \sin^2\theta \cos^2\varphi W_2$ reduces to the photoproduction cross section by a γ-ray beam with degree of polarization ϵ along the direction of motion.

H. F. Jones [2] has worked out the formuli connecting the W_i's with the center of mass amplitudes. We will rewrite his results in terms of ours $\mathcal{F}$'s:

$$W_1 = \frac{q}{k}\left[|\mathcal{F}_1|^2 + |\mathcal{F}_2|^2 - 2\cos\theta\ \mathrm{Re}(\mathcal{F}_1\mathcal{F}_2^*)\right] + \sin^2\theta\, W_2 \tag{3.4}$$

$$W_2 = \frac{1}{2}\frac{q}{k}\left[|\mathcal{F}_3|^2 + |\mathcal{F}_4|^2 + 2\,\mathrm{Re}(\mathcal{F}_2\mathcal{F}_3^* + \mathcal{F}_1\mathcal{F}_4^* + \cos\theta\,\mathcal{F}_3\mathcal{F}_4^*)\right] \tag{3.5}$$

$$W_3 = \frac{q}{k}\left(\frac{-\lambda^2}{k^2}\right)^{\frac{1}{2}}\mathrm{Re}\left[(\mathcal{F}_1 + \mathcal{F}_4 + \cos\theta\,\mathcal{F}_3)\,\mathcal{F}_7^* + (\mathcal{F}_2 + \mathcal{F}_3 + \cos\theta\,\mathcal{F}_4)\,\mathcal{F}_8^*\right] \tag{3.6}$$

$$W_4 = \frac{q}{k}\left(\frac{-\lambda^2}{k^2}\right)\left[|\mathcal{F}_7|^2 + |\mathcal{F}_8|^2 + 2\cos\theta\,\mathrm{Re}(\mathcal{F}_7\,\mathcal{F}_8^*)\right] \tag{3.7}$$

W_2 and W_3 can be separated out in (3.1) by their characteristic azymmuthal distributions. W_1 and W_4 can be obtained by measuring the cross section at different electron angles (different ε's).

IV - RESULTS ON THE ANGULAR DISTRIBUTION FOR π^+ AND π^o PRODUCTION

The separate study of the angular distributions W_1, W_2, W_3 and W_4 can lead to a much better understanding of the T-matrix. As was amphasized by Jones [2] one can study possible resonance behaviour of the multipoles both in their transverse and longitudinal excitations. Also some of the W_i may show a larger sensitivity to variations on the values of a given form factor and can serve as a check for more direct measurements.

According to eqs. (2.6), (2.7) and (2.8) the T-matrix depends linearly on the form factors. For low momentum transfer their values are reasonably well known except for the pion form factor, F_π and the neutron charge form factor, G_{eN}. Only the π^+-cross section depends on G_{eN}. For values of W around the first resonance and for momentum transfers less than $15f^{-2}$ the dependence on G_{eN} occurs mostly in W_1. To show this behaviour explicitly we have plot in fig. 4 the angular distributions for $\lambda^2 = -6f^{-2}$ and W = = 1230 MeV. We have fixed $F_\pi = 0.65$ (a value close to F_{1V}) and set $G_{eN} = 0.1$ and -0.1. One sees that the variation in G_{eN} produces essentially a change in scale.

The dependence of W_i on the pion form factor comes from two

sources: a) the resonant terms in Eq. (2.6), (2.7) and (2.8) which are model dependent and contribute for both π^o and π^+ production and b) the meson current diagram which contributes only for π^+-production. The meson current diagram has a pole in $\cos\theta$ at

$$\cos\theta = -(\lambda^2 - 2 q_o k_o)/2qk \qquad (4.1)$$

For sufficiently high energy the pole is very close to the physical region and makes a large contribution to the scalar part W_4 in the forward direction [14]. As we will show below the angular distribution W_4 is very sensitive to variations on F_π in the region of small angles. The Cornell group [1] took advantage of this behavior for estimating F_π. They fixed W, λ^2 and the pion scattering angle $\theta = 0$ and measured the cross section at different values of the electron scattering angle. At $\theta = 0$ (3.1) reduces to:

$$\frac{1}{\Gamma}\,\frac{d\sigma}{d\Omega_e^L\, dk_2^L\, d\Omega_\pi} = W_1 + \epsilon W_2 \qquad (4.2)$$

For ϵ variable (4.2) is a straight line. In fig. 5 we show the Cornell [1] results together with the predictions of our theory. For the nucleon form factors we use the values given by the Harvard 4-pole fit [15]. The value at $\epsilon = 0$ and at $\epsilon = 1$ gives the transverse part and the sum of the transverse and scalar parts, respectively. Of course one should not draw a sharp conclusion on the value of the pion form factor both due to the theoretical and experimental uncertainties. Although the theoretical predictions have been checked with relative success in photoproduction only total cross sections in the electroproduction case have been

compared with experiment until now. Also the values predicted by the theory depend on the values for the nucleon form factors which carry some uncertainties. As Frazer [4] pointed out a better procedure to obtain a value for F_π would be to extrapolate to the pion pole. We would like to remark that the extrapolations should be done in a region where the scalar contribution is large or, if experimentally feasible, in the scalar part only. The reason is that at $\theta = 0$ the one meson exchange diagram contribution vanish for the transverse part while it dominates the behavior of the scalar part.

Below we will give numerical predictions for W_1, W_2, W_3 and W_4. We have plot the angular distributions for two values of $\lambda^2 = -3f^{-2}$ and $-10f^{-2}$ and three values of W = 1175 MeV, 1230 MeV and 1300 MeV. To show the sensitivity of the various terms to variations on the pion form factor we set $F_\pi = 0.0$, 1.0 and to a value close to F_{1V} (0.8 for $\lambda^2 = -3f^{-2}$ and 0.5 for $\lambda^2 = -10f^{-2}$).

In figs. (6) to (9) we show the W_1, W_2, W_3 and W_4 angular distributions for π^+ production. The pure transverse terms, W_1 and W_2 show the same general behavior as their counterpart in photoproduction. The dependence on F_π comes from the meson current diagram and from the final state interactions. The first tends to show more in the high energy region. The scalar part, W_4, shows a large sensitivity for variations on F_π. The characteristic forward peak is due almost entirely to the meson current term. For this reason we believe that this is the term that can give the most reliable estimates of F_π. The transverse-scalar

interference is also quite sensitive to F_π.

According to our model the π^o-production amplitudes do not depend on G_{oN}. However, although the meson current term is not present, there is a dependence on F_π through the final state interaction in the 3-3 state.

At $\theta = 180^o$, eq. (4.2) is valid. In fig. 10 we compare the predictions of our theory with the Cornell's results for (4.2) at $\theta = 180^o$. The theoretical results obtained are larger than the experimental ones. In A the same overestimation at this angle appears in the case of photoproduction. This is due to the interference between the M_{1+} magnetic transition to the (3,3) state and the large E_{o+} obtained from the Born terms. Although important corrections to E_{o+} were made in A they are not large enough to explain the data well.

Figs. (11) to (14) are examples of angular distributions for the several terms in the cross section. Although the curves show a dependence on the values of F_π, one should be very careful in using them for estimating this quantity. Here the sensitivity comes from the resonant amplitudes and the values obtained will depend on the model used in the calculation.

FIGURE CAPTIONS

Fig. 1 - One photon exchange approximation in Electroproduction.

Fig. 2 - Born Terms: a) Direct nucleon pole diagram; b) Crossed nucleon pole diagram; c) Meson-pole diagram.

Fig. 3 - a) ρ-exchange diagram; b) ω-exchange diagram.

Fig. 4 - Angular distributions in the center of mass system for $\lambda^2 = -6f^{-2}$, W = 1230 MeV. The curves are drawn for G_{eN} = + 0.1 and - 0.1.

Fig. 5 - π^+-production. Comparison of Cornell's results and our prediction for $\theta = 0^\circ$. a) $\lambda^2 = -3f^{-2}$, W = 1175 MeV; b) $\lambda^2 = -3f^{-2}$, W = 1212 MeV; c) $\lambda^2 = -3f^{-2}$, W = 1313 MeV; d) $\lambda^2 = -6f^{-2}$, W = 1175 MeV. The curves are drawn for different values of F_π.

Fig. 6 - π^+-production. Transverse angular distribution $W_1(\theta)$. a) $\lambda^2 = -3f^{-2}$ and F_π = 1.0, 0.8 and 0.0; b) $\lambda^2 = -10f^{-2}$ and F_π = 1.0, 0.5 and 0.0.

Fig. 7 - π^+-production. Transverse angular distribution $W_2(\theta)$. a) $\lambda^2 = -3f^{-2}$ and F_π = 1.0, 0.8 and 0.0; b) $\lambda^2 = -10f^{-2}$ and F_π = 1.0, 0.5 and 0.0.

Fig. 8 - π^+-production. Transverse longitudinal interference angular distribution $W_3(\theta)$. a) $\lambda^2 = -3f^{-2}$ and F_π = 1.0, 0.8 and 0.0; b) $\lambda^2 = -10f^{-2}$ and F_π = 1.0, 0.5 and 0.0.

Fig. 9 - π^+-production. Longitudinal angular distribution $W_4(\theta)$. a) $\lambda^2 = -3f^{-2}$ and F_π = 1.0, 0.8 and 0.0; b) $\lambda^2 = -10f^{-2}$ and F_π = 1.0, 0.5 and 0.0.

Fig. 10 - π^0-production. Comparison of Cornell's results and our prediction for $\theta = 180^\circ$. a) $\lambda^2 = -3f^{-2}$, W = 1175 MeV; b) $\lambda^2 = -3f^{-2}$, W = 1200 MeV; c) $\lambda^2 = -3f^{-2}$, W = 1302 MeV; d) $\lambda^2 = -6f^{-2}$, W = 1175 MeV. The curves are drawn for different values of F_π.

Fig. 11 - π^0-production. Transverse angular distribution $W_1(\theta)$. a) $\lambda^2 = -3f^{-2}$ and F_π = 1.0, 0.8 and 0.0; b) $\lambda^2 = -10f^{-2}$ and F_π = 1.0, 0.5 and 0.0.

Fig. 12 - π^0-production. Transverse angular distribution $W_2(\theta)$. a) $\lambda^2 = -3f^{-2}$ and F_π = 1.0, 0.8 and 0.0; b) $\lambda^2 = -10f^{-2}$ and F_π = 1.0, 0.5 and 0.0.

Fig. 13 - π^0-production. Transverse longitudinal interference angular distribution $W_3(\theta)$. a) $\lambda^2 = 3f^{-2}$, and F_π = 1.0, 0.8 and 0.0; b) $\lambda^2 = -10f^{-2}$ and F_π = 1.0, 0.5 and 0.0.

Fig. 14 - π^0-production. Longitudinal angular distribution $W_4(\theta)$. a) $\lambda^2 = -3f^{-2}$ and F_π = 1.0, 0.8 and 0.0; b) $\lambda^2 = -10f^{-2}$ and F_π = 1.0, 0.5 and 0.0.

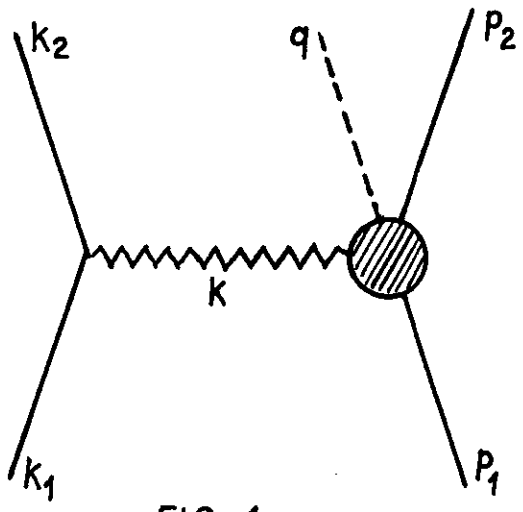

FIG. 1

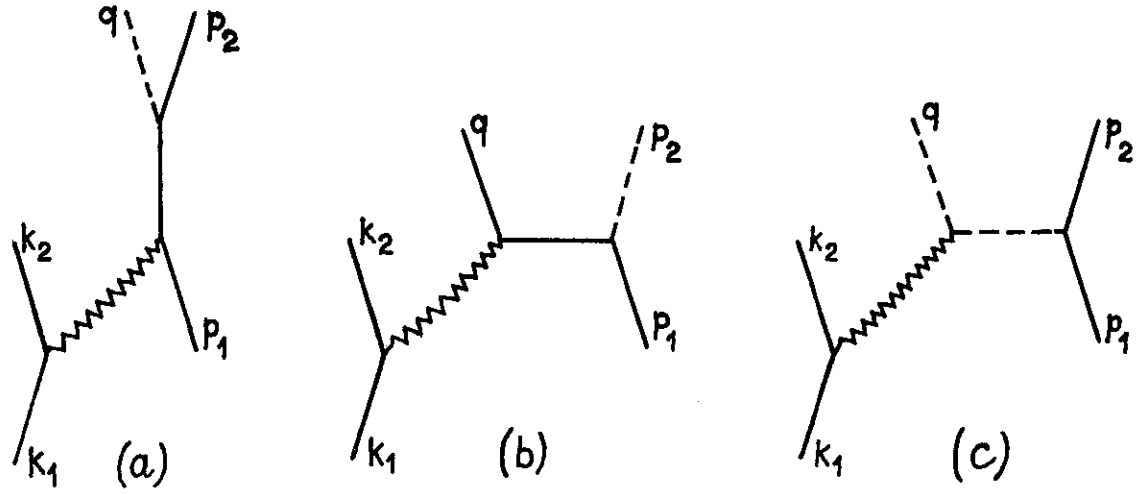

FIG. 2

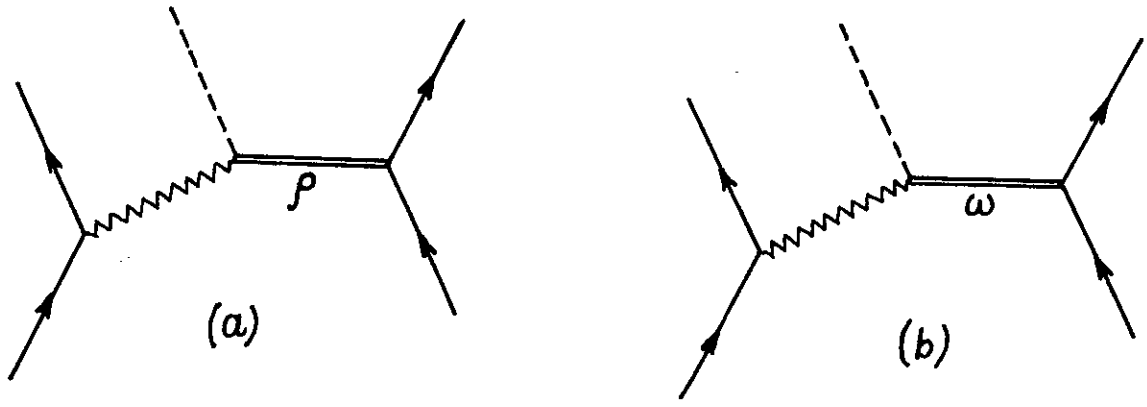

FIG. 3

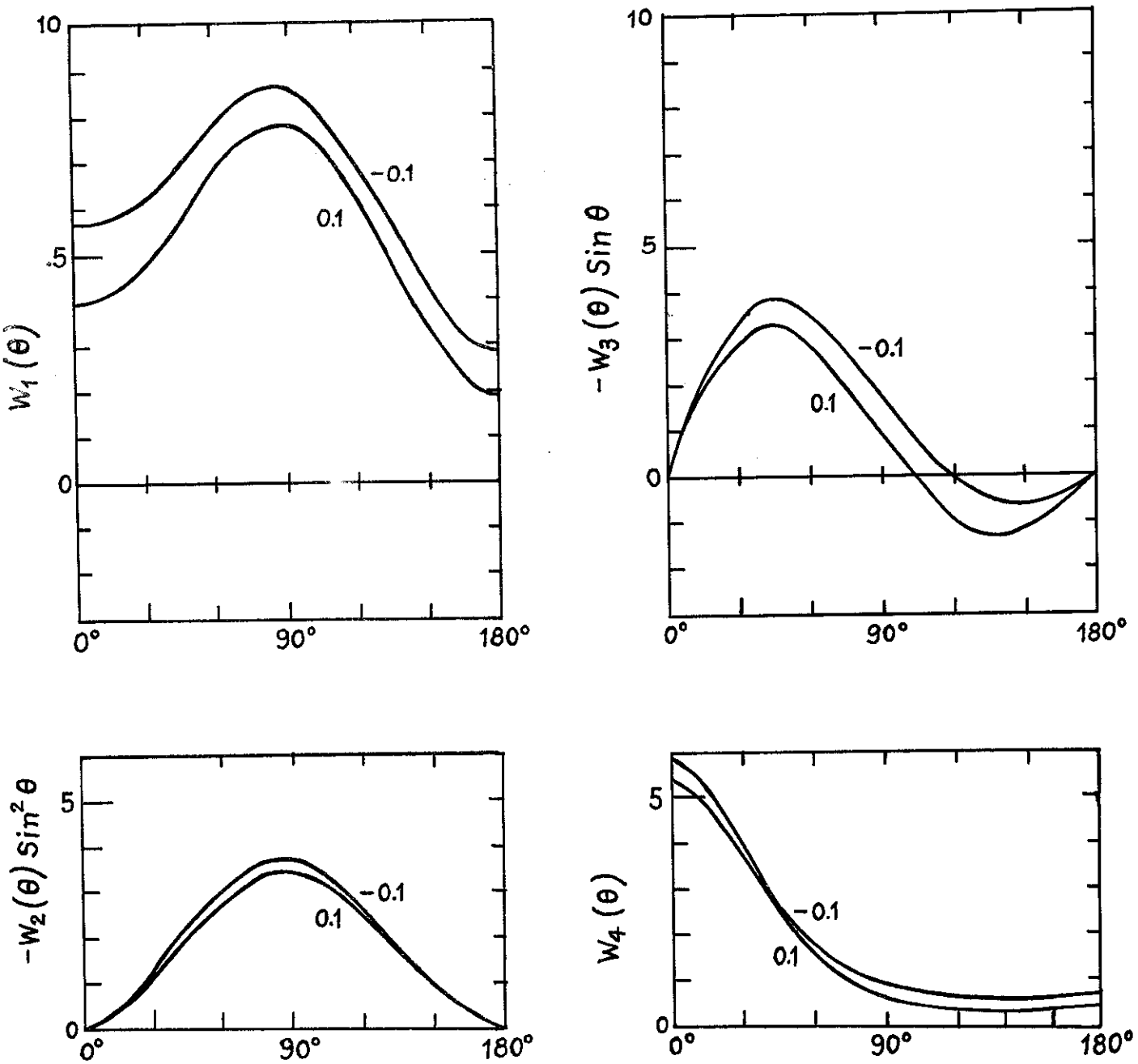
10
5
0
$W_1(\theta)$
-0.1
0.1
0°
90°
180°
10
5
0
$-W_3(\theta)\sin\theta$
-0.1
0.1
0°
90°
180°
5
0
$-W_2(\theta)\sin^2\theta$
-0.1
0.1
0°
90°
180°
5
0
$W_4(\theta)$
-0.1
0.1
0°
90°
180°

FIG. 4

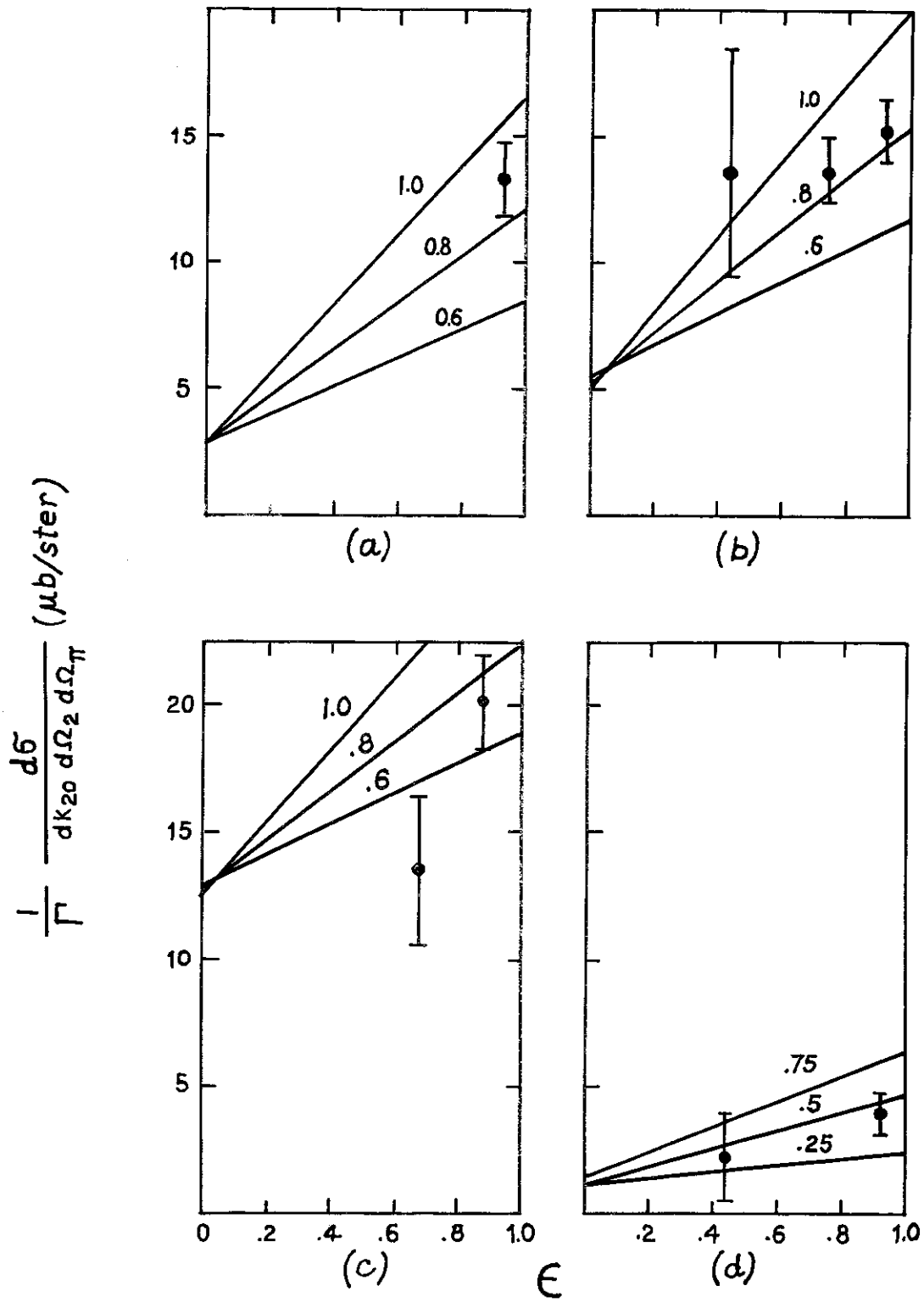
15
10
5
1.0
0.8
0.6
(a)
1.0
.8
.6
(b)
20
15
10
5
1.0
.8
.6
0
.2
.4
.6
.8
1.0
(c)
.75
.5
.25
.2
.4
.6
.8
1.0
(d)
ϵ
$\frac{1}{\Gamma}\frac{d\sigma}{dk_{20}\,d\Omega_2\,d\Omega_\pi}$ (μb/ster)

FIG. 5

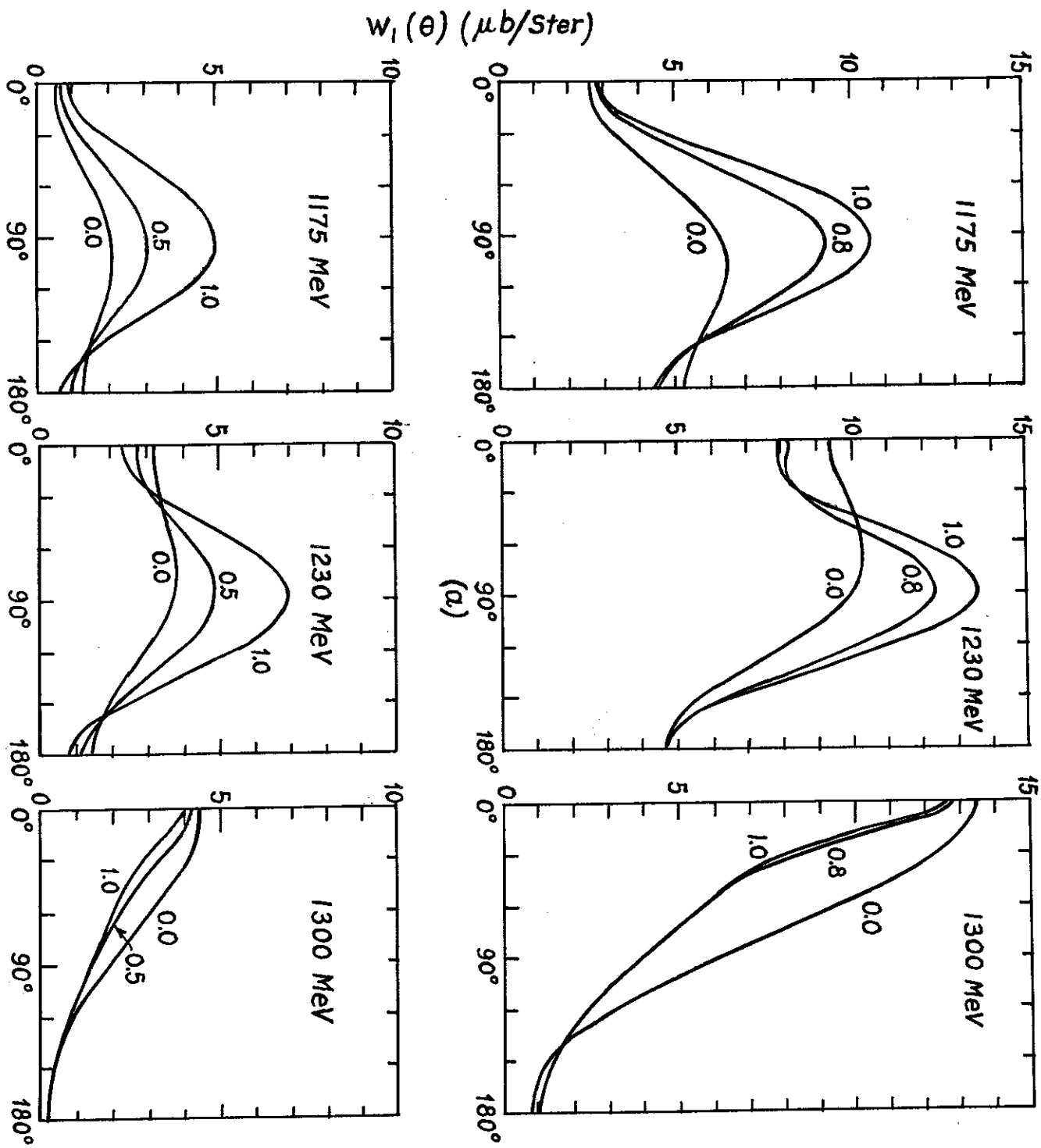
$W_1(\theta)$ (μb/Ster)
1175 MeV
1230 MeV
1300 MeV
0.0
0.5
0.8
1.0
(a)
0°
90°
180°

FIG. 6

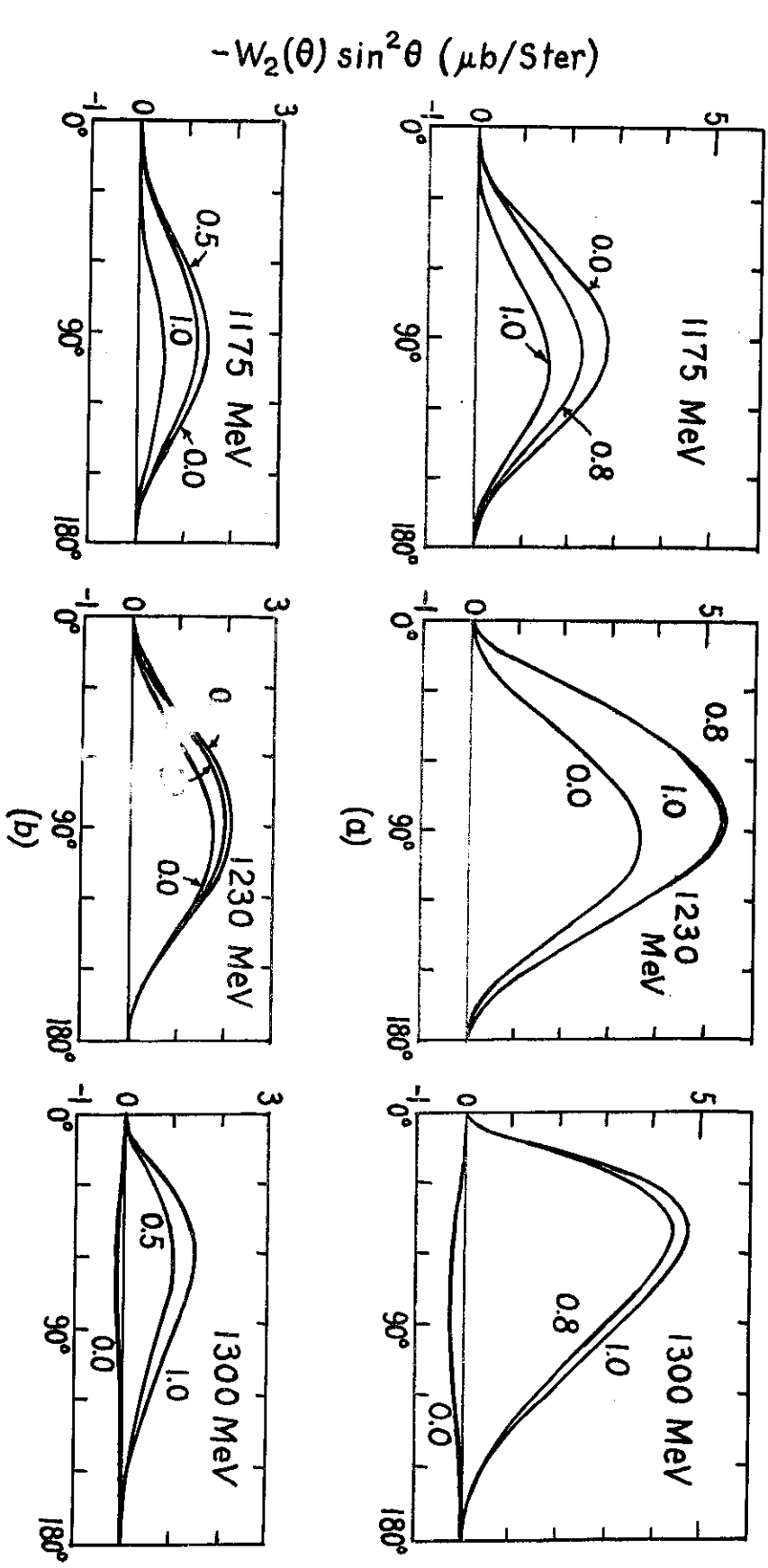
$-W_2(\theta)\sin^2\theta$ (μb/Ster)
1175 MeV
0.0
1.0
0.8
1175 MeV
0.5
1.0
0.0
(a)
1230 MeV
0.8
0.0
1.0
(b)
1230 MeV
0
0.0
1300 MeV
0.8
1.0
0.0
1300 MeV
0.5
0.0
1.0
-1
0
3
5
0°
90°
180°

FIG. 7

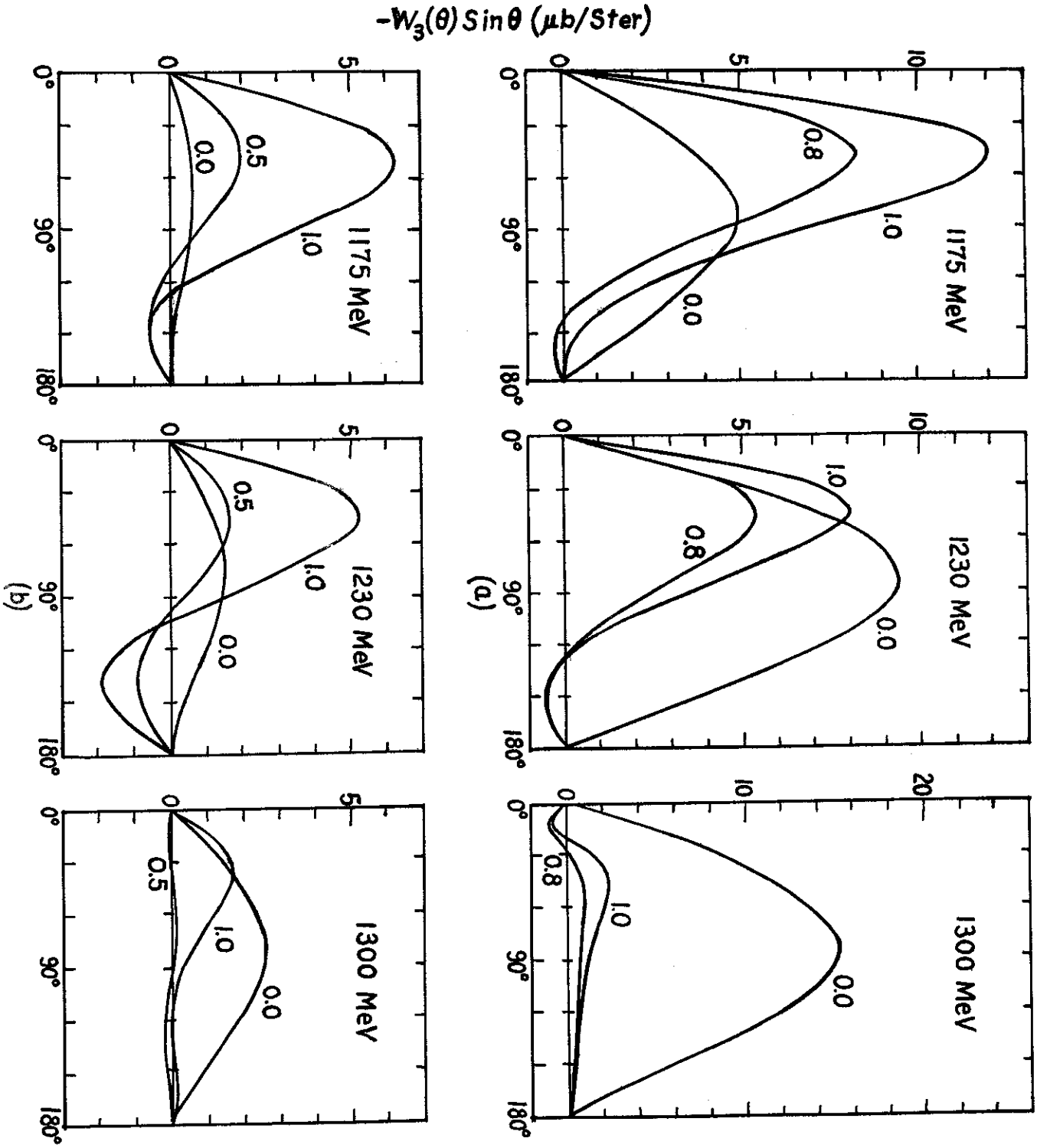
$-W_3(\theta)\,\sin\theta$ (μb/Ster)
1175 MeV
1230 MeV
1300 MeV
0.0
0.5
0.8
1.0
0°
90°
180°
(a)
(b)

FIG. 8

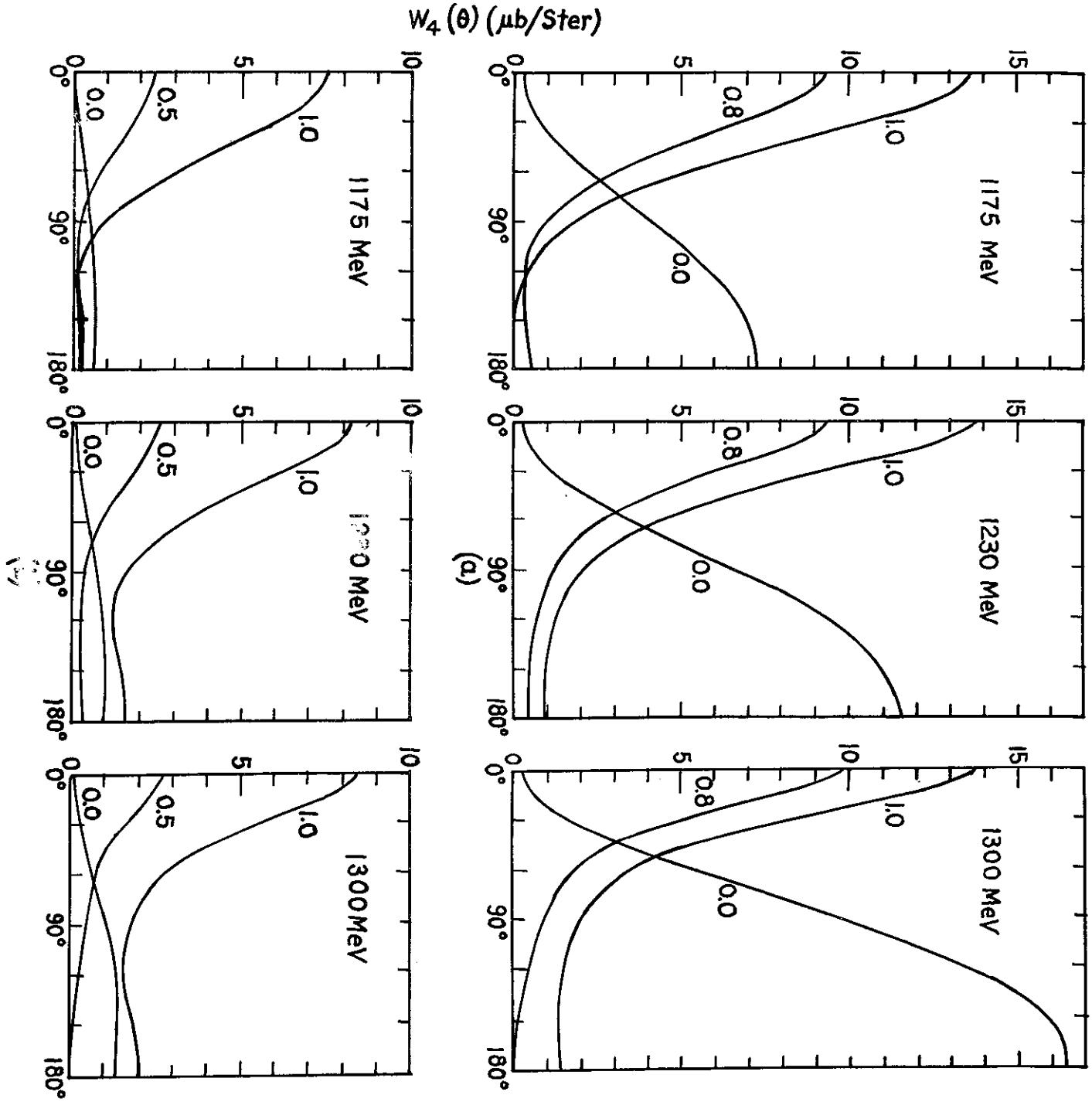

FIG. 9

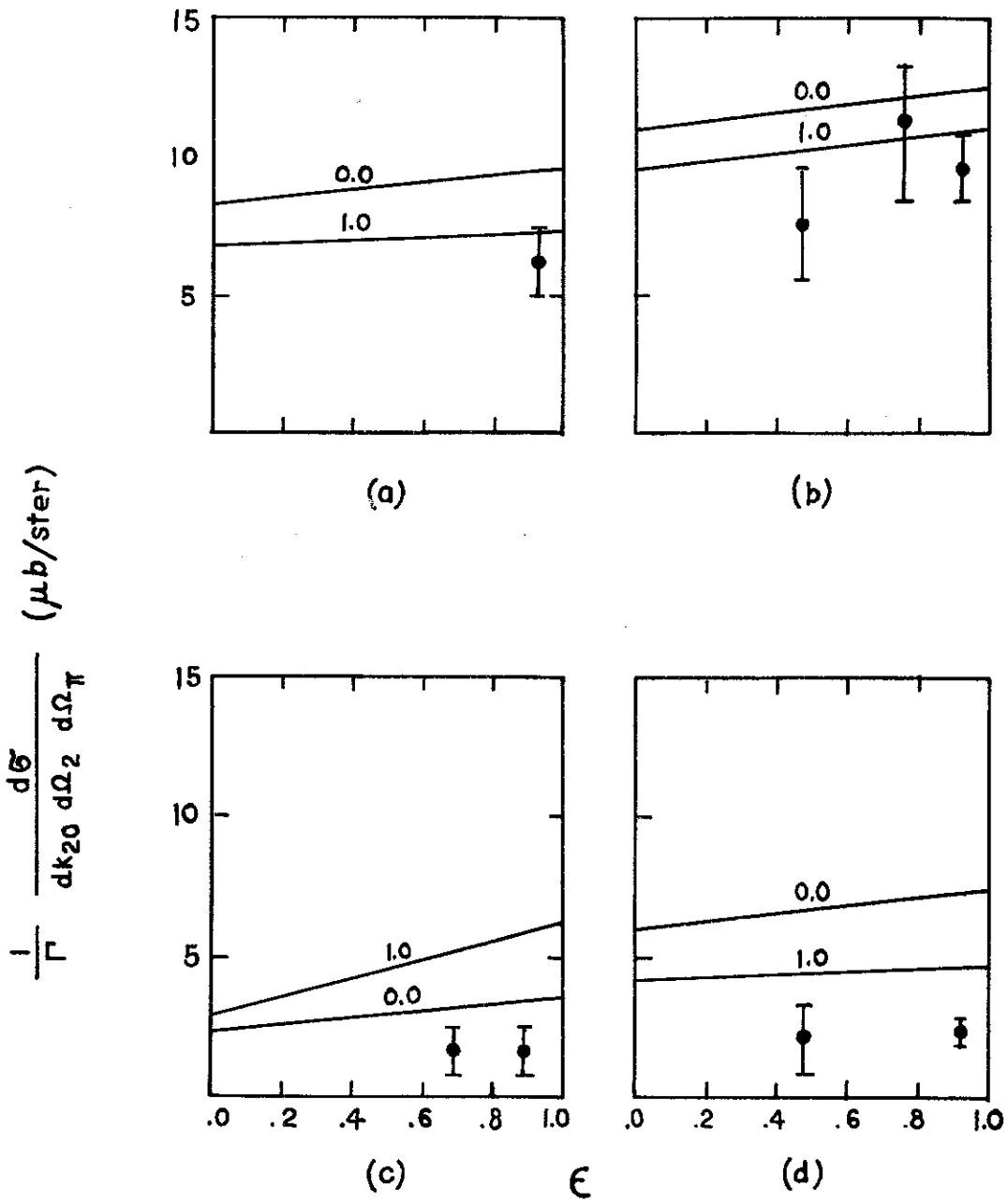
15
10
5
0.0
1.0
(a)
(b)
(c)
(d)
.0
.2
.4
.6
.8
1.0
ϵ
$\frac{1}{\Gamma}\frac{d\sigma}{dk_{20}\,d\Omega_2\,d\Omega_\pi}$ (μb/ster)

FIG. 10

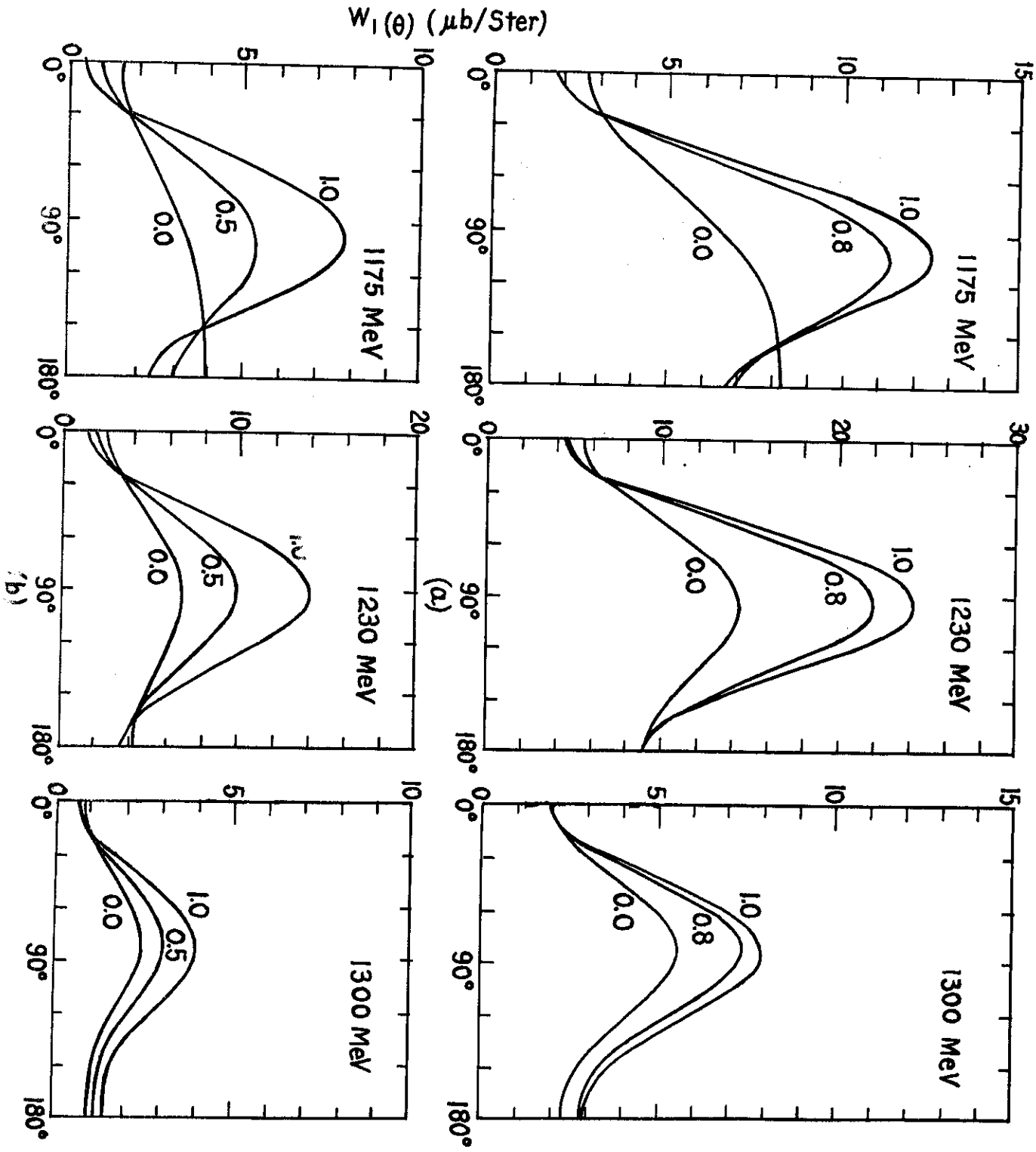

FIG. 11

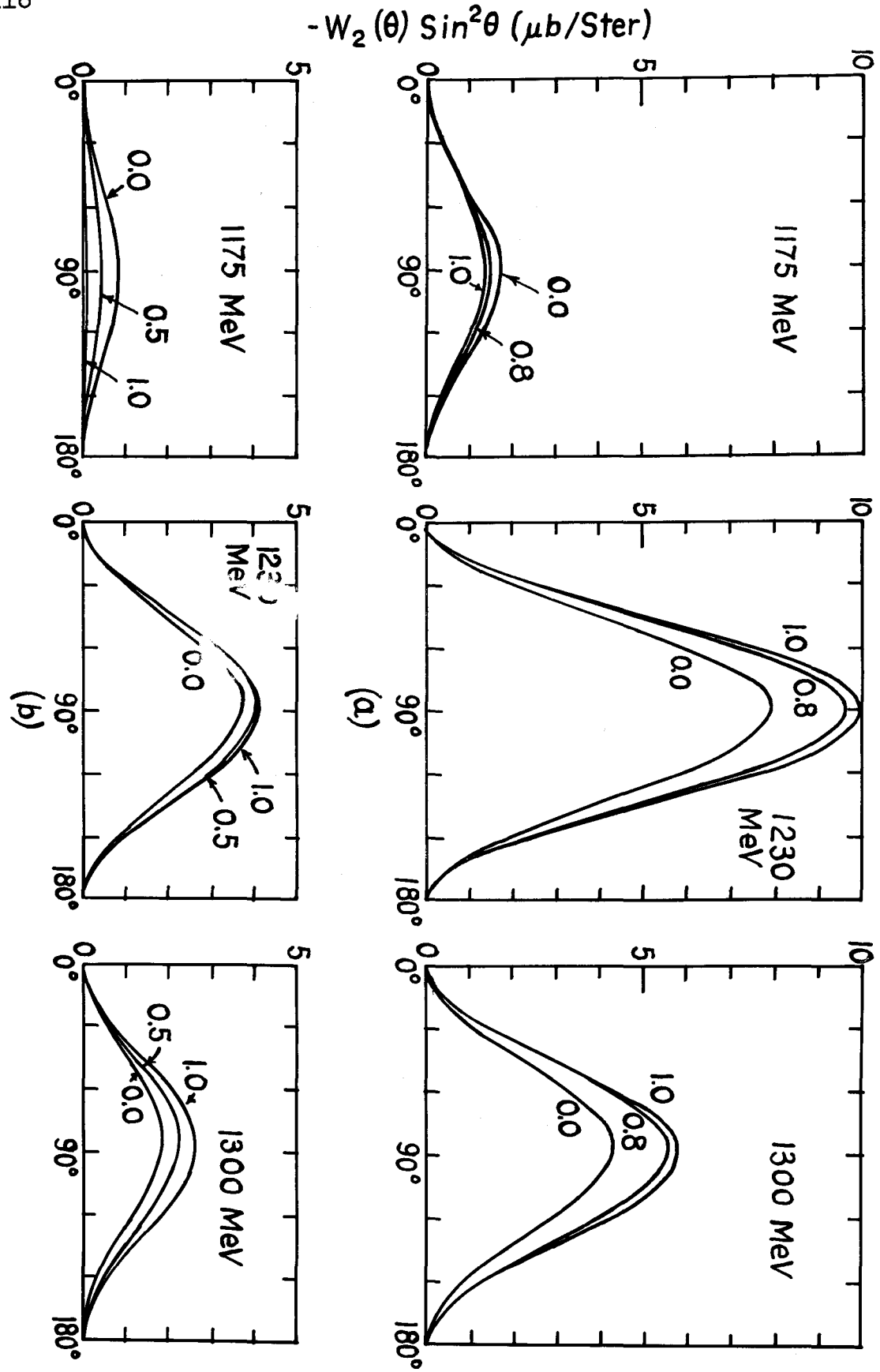
$-W_2(\theta)\ \sin^2\theta\ (\mu b/Ster)$
(a)
(b)
1175 MeV
1230 MeV
1300 MeV
0.0
0.5
0.8
1.0
0°
90°
180°
5
10

FIG. 12

1175 MeV
1230 MeV
1300 MeV
1.0
0.8
0.0
0.5
9
5
0
-3
-5
0°
90°
180°
(a)
(b)
$-W_3(\theta)\sin\theta$ (μb/Ster)

FIG. 13

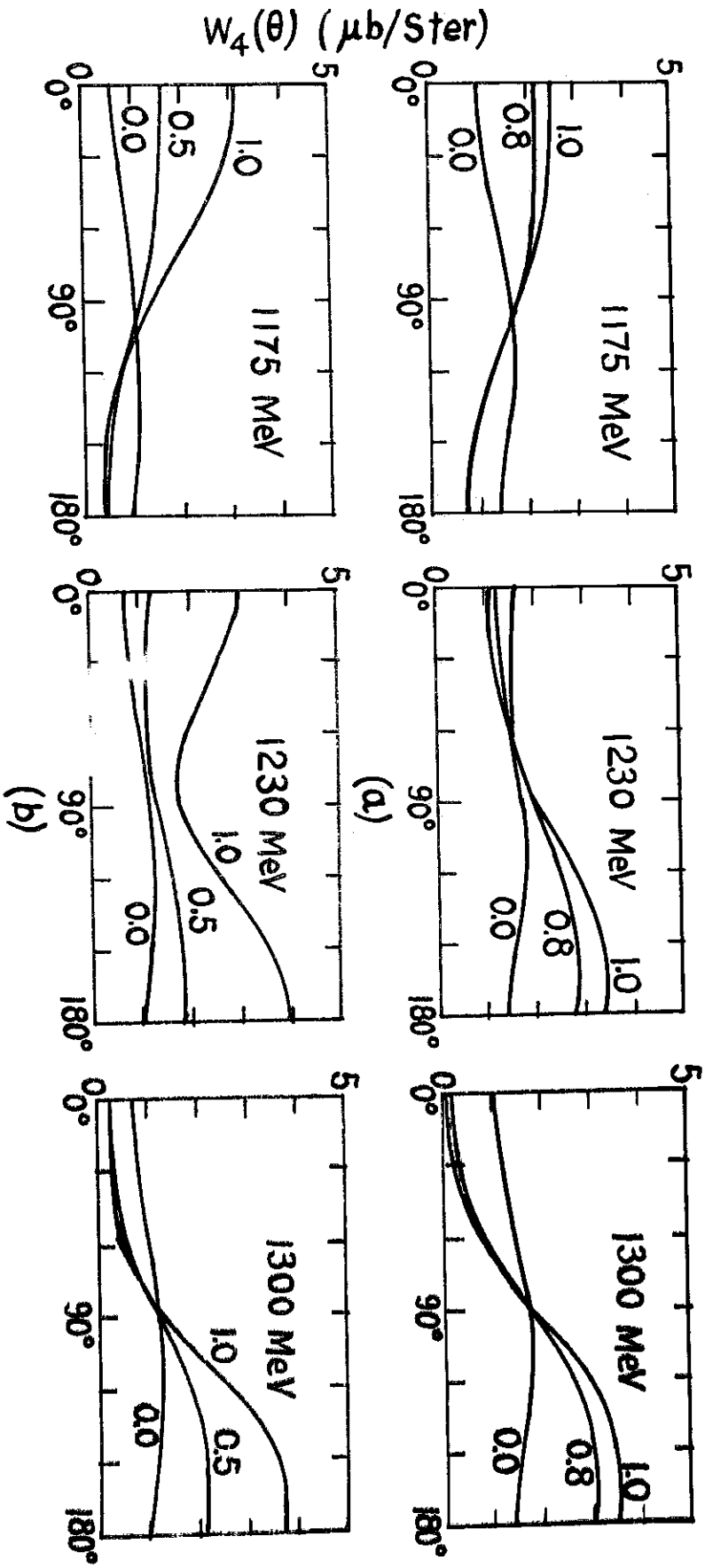
$W_4(\theta)$ (μb/Ster)
0°
90°
180°
5
0.0
0.5
1.0
0.8
1175 MeV
1230 MeV
1300 MeV
(a)
(b)

FIG. 14

REFERENCES

1. C. W. Akerlof, W. W. Ash, K. Berkelman and C. A. Lichtenstein, Phys. Rev. Letters 16, 147 (1966), C. W. Akerlof, W. W. Ash, K. Berkelman, C. A. Lichtenstein, A. Ramanauskas and R. H. Siemann, Proceedings of the 1966 International Conference on High Energy Physics at Berkeley, California (unpublished).
2. Here transverse and longitudinal refers to the polarization of the virtual photon in the one photon exchange approximation.
3. H. F. Jones, Nuovo Cimento 40, 1018 (1965).
4. W. R. Frazer, Phys. Rev. 115, 1736 (1959).
5. S. Fubini, Y. Nambu and V. Wataghin, Phys. Rev. 111, 329 (1958), P. Dennery, Phys. Rev. 124, 2000 (1961), S. L. Adler, Proceedings of the International Conference in Weak Interactions, Argonne National Laboratory (1965).
6. N. Zagury, Phys. Rev. 145, 1112 (1966). Hereafter referred to as A.
7. We are using the metric $g_{oo} = - g_{11} = - g_{22} = - g_{33} = 1$.
8. The scalar multipoles S is related to the longitudinal multipole L by $S = kL/k_o$. In A there are some misprints in the signs of the electric and scalar (3,3) multipoles.
9. J. S. Ball, A. Scotti and D. Wong, Phys. Rev. 142, 1000 (1966).
10. See, for example the R. H. Dalitz lectures at the 1965 Les Houches Summer School, eddited by de Witt and Jacob.
11. C. Badier and C. Bouchiat, Phys. Letters, 15, 96 (1965).
12. J. S. Ball, Phys. Rev. 124, 2014 (1966), A. Donachie and G. Shaw, Ann. Phys. 37, 333 (1966).
13. G. Fidecaro, M. Fidecaro, J. A. Poirier and P. Schiavon, Phys. Letters 23, 163 (1966), F. R. Hudson, J. F. Allard, D. Drijard, J. Hennessy, A. Lloret, J. Six and J. J. Veillet, Phys. Letters 20, 91 (1966).
14. The contribution for W_1 vanish at $0 = 0^o$.
15. L. H. Chan, K. W. Chen, J. R. Dunning, N. F. Ramsey, J. K. Walker and R. Wilson, Phys. Rev. 141, 1267 (1966).

* * *